# Surface Functionalization of ZnO Photocatalysts with Monolayer ZnS

2 **AUTHORS**, INCLUDING:

Matthias Batzill
University of South Florida
**116** PUBLICATIONS **4,369** CITATIONS

# Surface Functionalization of ZnO Photocatalysts with Monolayer ZnS

## Jayeeta Lahiri and Matthias Batzill*

*Department of Physics, University of South Florida, Tampa, Florida 33620*

*Received: December 3, 2007; In Final Form: January 10, 2008*

A fundamental investigation of the interface properties of coupled semiconductor photocatalysts in view of enhancing visible light activity is presented. We show by photoemission spectroscopy that modification of ZnO with submonolayer films of ZnS, two materials with band gaps larger than 3.4 eV, results in an effective surface band gap narrowing to 2.8 eV. This reduces the photoexcitation threshold energy and thus potentially enhances the solar energy conversion capabilities of such a heterostructure photocatalysts. Furthermore, the characterization of the space charge region and work function of ZnS modified ZnO indicate improved surface properties for enhancing photocatalytic activity.

## 1. Introduction

Photochemical solar energy conversion is a potential source of renewable energy. Production of chemical fuels over photocatalysts[1] and generation of electricity in electrochemical cells[2] are promising approaches. Transition metal oxides, for example $TiO_2$ or ZnO, are often used because they combine high photo activity with photostability.[3] However, these are wide band gap materials, 3.2 and 3.4 eV for $TiO_2$ and ZnO, respectively, and this limits their photo activity to the UV-range of the solar spectrum. Thus significant effort has been devoted to increase the activity of these materials by bulk doping[4−8] or functionalizing of their surfaces with narrow band gap inorganic quantum dots (QD)[9−11] or organic dye molecules.[2] In these materials, the surface groups have a narrow band gap and photoexcited electron−hole pairs are separated at the interface, injecting the electron into the metal oxide and leaving the hole at the surface. Subsequently the hole is transferred to a donor molecule from the gas phase or solution. For this mechanism to work efficiently the relative band alignment between the functional group and the substrate as well as the redox potential of the donor molecule are critical.[12]

One challenge for the surface functionalization is that many of the narrow band gap materials are susceptible to photo degradation and thus reducing the lifetime of photo devices.[13] Furthermore, many QD materials, such as CdS, consist of toxic materials that are not acceptable in certain applications. Here we propose a different approach for functionalizing the surface of ZnO to decrease the threshold energy for photoexcitation. ZnO is modified with a (sub) monolayer of ZnS. ZnS by itself is known to be an efficient photocatalyst,[14] however, it faces the same limitation as ZnO due to its even wider bulk band gap (3.7 eV). Here we show that although ZnO and ZnS have a high photo energy threshold by themselves at the ZnO/ZnS interface the band alignment is favorable for reducing the photoexcitation threshold energy. Hence, the combination of two wide band gap photocatalysts can yield a material with lower photoexcitation threshold than the individual components. Furthermore, we show that less than a monolayer of ZnS suffices to achieve this beneficial effect. Such a small amount of ZnS

can be easily stabilized in a slightly sulfidizing solution[3] and thus for practical reasons ensure a long lifetime of this modified ZnO photocatalyst.

The concept of coupled semiconductor photocatalysts for the purpose of increasing electron−hole separation by formation of interface contact potentials have been studied for numerous materials combination.[15−24] In some of these systems an extension of the photoresponse range has also been reported. Generally these photocatalysts are complex micro-structured materials, which make a fundamental investigation of the interface properties challenging. Here we pursue a surface science approach on single-crystal ZnO. This enables us to investigate the fundamental interface properties between ZnS and ZnO as a model system for coupled semiconductor photocatalysts and to demonstrate the materials modifications that allow tuning the photo catalytic properties in such hetero systems. It is anticipated that a better understanding of these interface properties will assist the controlled design of multi-component photocatalysts of the future.

## 2. Experimental Methods

The studies were performed on single-crystal ZnO wafers with polar orientation. Both polar surfaces, i.e., (0001) and (000$\bar{1}$) were studied.[25] The band alignment at the ZnS/ZnO interface was very similar for the two surfaces and therefore, for brevity, we only discuss the (0001) surface, i.e., the Zn-terminated side. Photoemission studies were performed at the U12a beamline at the National Synchrotron Light Source. This beamline is optimized for soft X-ray photoemission spectroscopy with a photon energy range between 1 and 0.1 keV which enables acquisition of both core-level and valence band photoemission spectra. The photon-energies were calibrated by measuring second-order light induced photoemission peaks as well as measuring the Fermi-edge on the metal sample holder. The work function of the sample was measured from the cutoff of the secondary electron background. For this measurement the samples were biased at −9 V to increase the kinetic energy of the low-energy electrons. Using the known analyzer work function, the absolute sample work function could be determined.

Scanning tunneling microscopy (STM) studies of the surfaces were performed with a variable (high) temperature Omicron

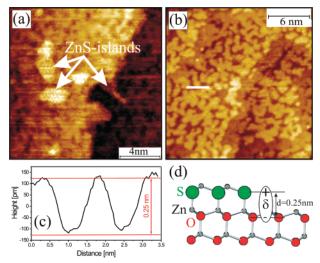* To whom correspondence should be addressed. E-mail: mbatzill@cas.usf.edu.

Surface Functionalization of ZnO Photocatalysts

*J. Phys. Chem. C, Vol. 112, No. 11, 2008* **4305**



**Figure 1.** STM images of sulfur induced surface structure for (a) 0.6 L $H_2S$ and (b) 3 L $H_2S$ exposure. The cross-section indicated in (b) is shown in (c). A ball-and-stick model of the surface structure is shown in (d) with the surface dipole moment indicated.



**Figure 2.** Summary of the changes in the work function, valence band maximum (relative to the Fermi level), band bending in the substrate, and the $S_{2p}/Zn_{3s}$ peak ratios as a function of $H_2S$ exposure are shown. All properties saturate between 3 and 6 L $H_2S$ exposure.

STM. Images were acquired at ~550 K to increase sample conductivity. All the sample preparation and characterization were performed in ultrahigh vacuum. Clean ZnO samples were prepared by cycles of ion sputtering and subsequent annealing to ~900 K. Sulfide films were grown by exposure of the ZnO surface to $H_2S$ at a sample temperature of 600 K. The sulfur exposures are given in Langmuir derived from the $H_2S$ pressure and exposure time. The $H_2S$ pressure was measured with an ion gauge and was not corrected for the sensitivity factor of the ion gauge for $H_2S$.

## 3. Results

The morphology of ZnS films on ZnO is crucial for interpretation of the fundamental electronic and thus photochemical surface properties. Therefore we discuss the surface morphology as found from STM studies first, followed by the electronic structure characterization derived from photoemission studies.

**3.1. Structural Surface Modifications.** ZnO is used for desulfurization of feedstock in catalysis and therefore is known to be easily sulfidized by $H_2S$.[26] However, little is known about the morphology of ZnS layers that form at the surface of ZnO. STM studies indicate that ZnS grows by nucleation and growth of 2D islands, of monolayer height (~ 2.5 Å). After exposure to 3−6 L $H_2S$ a dense network of meandering islands is formed. STM images of ZnO surface for low $H_2S$ exposure and for saturation $H_2S$ dose is shown in Figure 1, panels a and b, respectively. For such films the $S$-$2p^{3/2}$ core level is detected at a binding energy (BE) of 162.3 eV for low S-coverage and at 162.2 eV for a saturation dose. This BE is consistent with sulfide formation. However, the value is about 0.4 eV higher than that reported for bulk ZnS (161.8 eV).[27] Although the atomic scale structure of the sulfide film cannot be unambiguously deduced from our STM studies, some islands exhibit hexagonal symmetry. Therefore, it is reasonable to assume that ZnS adopts the wurtzite structure of the ZnO substrate and an epitaxial relationship between substrate and film is established. The much larger lattice constant of wurtzite-ZnS ($a = 3.82$ Å; $c = 6.26$ Å) compared to ZnO ($a = 3.25$ Å; $c = 5.21$ Å) implies that a complete ZnS monolayer would be under considerable compressive stress. Therefore the formation of the meandering island
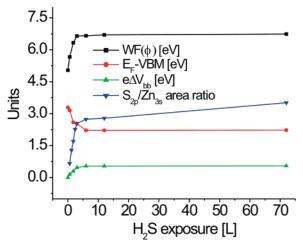
morphology is likely to be a strain relieve-mechanism of the film. The large strain, a complete ZnS film would have, implies an increase in the S-chemical potential with ZnS coverage and thus provides a reason for the saturation of the sulfur uptake before completion of the monolayer.

**3.2. Electronic Surface Modification.** In order to assess the influence of the submonolayer film on the fundamental surface properties and thus the photocatalytic properties the alterations of the electronic structure needs to be analyzed. Photoemission has been used to measure the electronic interface properties between ZnO and (sub) monolayer ZnS films. Experiments were performed for increasing $H_2S$ exposure. The results of these measurements are summarized in Figure 2. One graph shows the S-2p/Zn-3s peak ratios, which indicates that initially the surface coverage increases rapidly. At ~6L $H_2S$ a saturation of the surface phase is reached, subsequent increase in the S-2p intensity is slow. This behavior is in agreement with the STM studies that indicate a 2D island growth mode of ZnS. A similar behavior has also been reported for the ZnO(11$\bar{2}$0) surface.[28]

The core level peak positions for O-1s, Zn-3s, and 3d have been used for evaluating the band bending induced in the ZnO substrate by sulfur exposure. Figure 3a shows for example the Zn-3d core level position for different S-exposures. A shift of 0.55 eV to lower binding energies with increasing S-exposure is observed. This core level shift also saturates at 3−6 L exposure. A similar shift has been measured for the O-1s core level. These shifts can be attributed to an electrostatic upward band bending due to surface charge transfer.[29]

The valence band was monitored with a photon energy of 150 eV and this is shown in Figure 3 (b). In addition to a shift to lower binding energies of the valence band maximum (VBM) due to upward band bending, a new state is formed on top of the valence band in the band gap of ZnO. This state is due to the ZnS layer at the surface. This ZnS state can be clearer appreciated in difference spectra. In these spectra the spectrum of the clean ZnO surface has been shifted by the amount of band bending and subtracted from the spectra after $H_2S$ exposures. The top of the ZnS states are observed at 2.1−2.2 eV below the Fermi level. Interestingly, the onset of this state does not shift with S-coverage, indicating that the electronic properties of the growing ZnS film does not change significantly with coverage. This is contrary to what one would expect for a strained film.
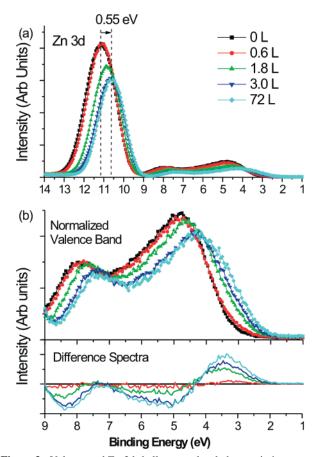
**Figure 3.** Valence and Zn-3d shallow core level photoemission spectra for different H$_2$S exposures. The band bending induced shift in the Zn-3d core level can be observed in (a). The change in the valence band is shown in (b). The difference spectra are calculated by subtraction of the spectrum of the clean surface after shifting it to compensate for band bending effects.

The measurement of the work function indicates a large increase upon formation of the ZnS layer (see Figure 2b). For the clean ZnO (0001)-Zn surface we obtain a value of 5.0 eV (literature values for ZnO surfaces vary between 3.7 and 6 eV)[30] this value increases by 1.7 to 6.7 eV upon formation of the ZnS layer. This increase in work function has two contributions: (i) band bending, and (ii) surface dipole moment. After subtracting the upward band bending (0.55 eV) we arrive at a dipole induced increase in the work function of 1.15 eV. This indicates a surface dipole layer with the positive side toward the vacuum. A likely origin of this strong change lies in the larger electronegativity of O compared to S. Therefore in a layer model of ZnS on top of the ZnO substrate, as is shown in Figure 1d, charges from the ZnS surface are transferred to the ZnO substrate. Such a charge transfer is substantiated by the chemical shift of S-2p core level position to higher BE compared to the reported bulk ZnS value. Assuming a structure as indicated in Figure 1d we can estimate the dipole moment per surface S-atom to $\delta = 0.25$ D, or a corresponding charge transfer of 0.02 e per S-atom.

## 4. Discussion

By combining all the above measurements and using 3.4 eV for the ZnO band gap, the interface band diagram can be derived. This is shown in Figure 4. Due to electronic hybridization of the monolayer ZnS film with the ZnO substrate photoexcitation from the ZnS surface states to the ZnO conduction band are possible. Thus an effective band gap narrowing from 3.4 to 2.8
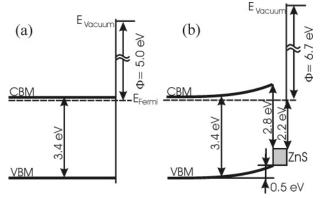


**Figure 4.** Schematic surface band diagram for (a) the clean ZnO-(0001) surface and (b) after formation of ZnS surface layer.

eV is observed at the interface. A similar band gap narrowing has been observed for S-doped ZnO[31] and may also be responsible for the reported green light photoluminescence[32−34] in S-doped ZnO nanomaterials.

A staggered band alignment between ZnO and ZnS was also recently predicted by DFT calculations.[35] However, our observed effective band gap of 2.7−2.8 eV is much larger than the predicted (1.82 eV) value. This is partially because a significant narrowing of the fundamental band gap in ZnO was predicted due to ZnS induced lattice strain. In our experimental studies of (sub) monolayer ZnS films we do not see any shift of the ZnS states with increasing coverage as one would expect if the strain in the film were to play an important role in the interface electronic structure. Therefore we propose that the formation of ZnS-island morphology provides an efficient strain relieve mechanism for pseudomorphic ZnS layers.

Apart from reducing the photoexcitation threshold to lower photon energy the electronic structure has several other implications for the use of this material for photochemical applications. The band bending at the surface will facilitate the electron−hole separation. Holes, on the other hand, will be trapped in the ZnS adlayer states that have a lower BE than the top of the ZnO valence band. Here the holes become available for charge transfer to a donor molecule in the gas phase or solution. The increase in work function will shift the redox potential of these adsorbed donor molecules to more negative values, i.e., to lower binding energies relative to the VBM. This will increase the thermodynamic driving force for charge transfer from donor molecules to holes trapped in the ZnS layer. All these alterations of the surface properties taken together will enhance hole-mediated photo catalytic reactions at the ZnS modified surface compared to the clean ZnO surface.

## 5. Conclusion

In conclusion, these studies demonstrate that surface functionalization of photoactive materials with a wide band gap material can result in an effective band gap narrowing at the surface. Other surface properties (work function and band bending) may also assist in increasing the photo activity. For large surface area nanomaterials, this surface modification with ZnS will increase the visible light photo absorption. The concurrent formation of hole trapping states at the surface and a space charge region that facilitates charge separation at the surface make this a promising materials system for demonstrating the potential for increasing visible light activity by combining two UV-active photocatalysts. Optimizing the ZnO/ZnS materials system by, e.g., increasing the strain in the interface layer or formation of multilayer heterostructures, may shift the

Surface Functionalization of ZnO Photocatalysts

*J. Phys. Chem. C, Vol. 112, No. 11, 2008* **4307**

photoexcitation threshold to even lower energies. Other material systems that combine wide band gap photocatalysts may exist that show similar favorable interface effects. Thus based on our fundamental materials characterization a new paradigm for designing more active photocatalysts, fundamentally different to surface functionalization by narrow band gap materials or bulk doping, is being suggested.

## References and Notes

(1) Fujishima, A.; Honda, K. *Nature* **1972**, *238*, 37.

(2) O'Regan, B.; Grätzel, M. *Nature* **1991**, *353*, 737.

(3) Kaneko, M., Okura, I., Eds.; *Photocatalysis; Science and Technology*; Springer: Berlin, 2002.

(4) Choi, W. Y.; Termin, A.; Hoffmann, M. R. *J. Phys. Chem.* **1994**, *84*, 13669.

(5) Anpo, M.; Dohshi, S.; Kitano, M.; Hu, Y.; Takeuchi, M.; Matsuoka, M. *Annu. Rev. Mater. Res.* **2005**, *35*, 1.

(6) Khan, S. U. M.; Al-Shahry, M.; Ingler, W. B., Jr. *Science* **2002**, *297*, 2243.

(7) Asahi, R.; Morikawa, T.; Ohwaki, T.; Aoki, K.; Taga, Y. *Science* **2001**, *293*, 269.

(8) Batzill, M.; Morales, E. H.; Diebold, U. *Phys. Rev. Lett.* **2006**, *96*, 026103.

(9) Chang, C. H.; Lee, Y. L. *Appl. Phys. Lett.* **2007**, *91*, 053503.

(10) Diguna, J. L.; Shen, Q.; Kobayashi, J.; Toyoda, T. *Appl. Phys. Lett.* **2007**, *91*, 023116.

(11) Leschkies, K. S.; Divakar, R.; Basu, J.; Enache-Pommer, E.; Boercker, J. E.; Carter, C. B.; Kortshagen, U. R.; Norris, D. J.; Aydil, E. S. *Nano Lett.* **2007**, *7*, 1793.

(12) Moons, E.; Eschel, M.; Grätzel, M. *Appl. Phys. Lett.* **1997**, *71*, 3305.

(13) Ozasa, K.; Maeda, M.; Hara, M. *Microelectr. J.* **2005**, *36*, 578.

(14) Tsuji, I.; Kato, H.; Kudo, A. *Angew. Chem., Int. Ed.* **2005**, *44*, 3565.

(15) Serpone, N.; Maruthamuthu, P.; Pichat, P.; Pelizzetti, E.; Hidaka, H. *J. Photochem. Photobiol. A* **1995**, *85*, 247.

(16) Shiyanovskaya, I.; Hepel, M. *J. Electrochem. Soc.* **1998**, *145*, 3981.

(17) Song, K. Y.; Park, M. K.; Kwon, Y. T.; Lee, H. W.; Chung, W. J.; Lee, W. I. *Chem. Mater.* **2001**, *13*, 2349.

(18) Yu, J. C.; Lin, J.; Kwok, R. W.M. *J. Phys. Chem. B* **1998**, *102*, 5094.

(19) Pal, B.; Sharon, M.; Nogami, G. *Mater. Chem. Phys.* **1999**, *59*, 254.

(20) Marci, G.; Augugliaro, V.; Lopez-Munoz, M. J.; Martin, C.; Palmisano, L.; Rives, V.; Schiavello, M.; Tilley, R. J. D.; Venezia, A. M. *J. Phys. Chem. B* **2001**, *105*, 1026.

(21) Bedja, I.; Kamat, P. V. *J. Phys. Chem.* **1995**, *99*, 9182.

(22) Bessekhouad, Y.; Robert, D.; Weber, J. V. *Catal. Today* **2005**, *101*, 315.

(23) Wang, C.; Wang, X.; Xu, B.-Q.; Zhao, J.; Mai, B.; Peng, P.; Sheng, G.; Fu, J. *J. Photochem. Photobio. A* **2004**, *168*, 47.

(24) Huang, T.; Lin, X.; Xing, J.; Wang, W.; Shan, Z.; Huang, F. *Mater. Sci. Eng. B* **2007**, *141*, 49.

(25) Wöll, C. *Prog. Surf. Sci.* **2007**, *82*, 55.

(26) Li, L. Y.; King, D. L. *Catal. Today* **2006**, *116*, 537.

(27) Rodriguez, J. A.; Li, S. Y.; Hrbek, J.; Huang, H. H.; Xu, G. Q. *J. Phys. Chem.* **1996**, *100*, 14476.

(28) Bech, M.; Simonsen, J. B.; Handke, B.; Li, Z.; Møller, P. J. *Surf. Sci.* **2006**, *600*, 3375.

(29) Liu, G.; Schulmeyer, T.; Thissen, A.; Klein, A.; Jaegermann, W. *Appl. Phys. Lett.* **2003**, *82*, 2269.

(30) Jacobi, K.; Zwicker, G.; Gutmann, A. *Surf. Sci.* **1984**, *141*, 109.

(31) Yoo, Y. Z.; Jin, Z. W.; Chikyow, T.; Fukumura, T.; Kawasaki, M.; Koinuma, H. *Appl. Phys. Lett.* **2002**, *81*, 3798.

(32) Zhou, P. L.; Yu, X. B.; Yang, L. Z.; Tao, Z. W. *Mater. Lett.* **2007**, *61*, 3870.

(33) Shen, G. Z.; Cho, J. H.; Jung, S. I.; Lee, C. *J. Chem. Phys. Lett.* **2005**, *401*, 529.

(34) Bae, S. Y.; Seo, H. W.; Park, J. *J. Phys. Chem. B* **2004**, *108*, 5206.

(35) Schrier, J.; Demchenko, D. O.; Wang, L.-W.; Alivisatos, A. P. *Nano Lett.* **2007**, *7*, 2377.